Polymer 293 (2024) 126636

Contents lists available at ScienceDirect

Polymer

journal homepage: www.elsevier.com/locate/polymer

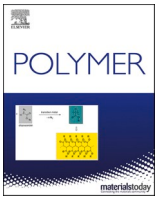

Exploiting β-amino ester chemistry to obtain methacrylate-based covalent adaptable networks

Chiara Ivaldi [a,c,*], Erica Laguzzi [b,c], Viviana Maria Ospina [b,c], Diego Antonioli [b,c], Riccardo Chiarcos [b,c], Federica Campo [d], Nicola Cuminetti [d], Janosc De Buck [d], Michele Laus [b,c,**]

[a] Dipartimento per lo Sviluppo Sostenibile e la Transizione Ecologica (DISSTE), Università del Piemonte Orientale "A. Avogadro'', Piazza S. Eusebio 5, 13100, Vercelli (VC), Italy
[b] Dipartimento di Scienze e Innovazione Tecnologica (DISIT), Università del Piemonte Orientale "A. Avogadro'', Viale T. Michel 11, 15121, Alessandria (AL), Italy
[c] INSTM, UdR Alessandria (AL), Italy
[d] ELANTAS Europe S.r.l., Via San Martino 6, 15028, Quattordio (AL), Italy

ARTICLE INFO

Keywords:
Covalent adaptable network (CAN)
β-amino ester (BAE)
Vitrimer
Methacrylate-based covalent adaptable network
Aza-michael addition
Neighbouring group participation (NGP)
Industrially relevant material
Shape memory
Reprocessing

ABSTRACT

In this study, β-amino ester-based covalent adaptable networks (CANs) were synthesised through aza-Michael addition of amines to methacrylates, with the aim of developing industrial products. Typically, CANs based on β-amino esters employ acrylate moieties, which are known to be toxic and hazardous to human health and the environment. Therefore, methacrylate-based networks were explored as a safer alternative to the chemistry currently in use. Network formation was monitored by following the evolution of the glass transition temperature over time and conducting soluble fraction tests. Subsequently, industrial methacrylic monomers were employed to develop an industrially relevant material, utilizing previously established curing conditions for methacrylate systems. The dynamic behaviour of the network was assessed through rheological characterisation. The material demonstrated the ability to relax applied stress at various temperatures displaying typical viscoelastic fluid behaviour, indicative of exchangeable linkages within the macromolecular architecture. Shape memory and reprocessing capability were successfully tested under appropriate thermo-mechanical stimulation. Both thermal analyses and FT-IR spectra confirmed the retention of chemical composition and material properties throughout recycling process.

1. Introduction

Since the 1950s, we have been living in the "Age of Plastic". Because of their wide range of industrial and household applications, polymeric materials have become essential in our daily lives [1,2]. Annually, more than 460 million tons of plastics are produced, yet only approximately 9 % of them are recycled [3]. Therefore, one of the most pressing issues of current times is the increasing amount of fossil-based plastic waste dispersed in the environment. In response, the adoption of a circular economy, involving reuse, repair, and recycling of existing materials is imperative for a sustainable lifestyle [4]. Nevertheless, recovering plastics presents various challenge [5] and thermosets are currently in the focus of scientific community in terms of end-of-life management. Designed intrinsically with a high cross-linked structure to be long-lasting and highly durable, thermosetting materials cannot indeed be thermally reprocessed or recycled without a loss of mechanical properties. Incineration or disposal in landfills [6] are their most common final destiny.

In the context of enhancing the recyclability and reusability of thermosets, a straightforward chemical approach involves incorporating dynamic covalent bonds within their macromolecular architecture. These covalent crosslinks become reversibly dynamic when an external stimulus is applied, such as heat [7], light [8], or pH [9]), enabling a molecular network rearrangement (MNR) process. This dynamic

* Corresponding author. Dipartimento per lo Sviluppo Sostenibile e la Transizione Ecologica (DISSTE), Università del Piemonte Orientale A. Avogadro, Piazza S. Eusebio 5, 13100, Vercelli (VC), Italy.
** Corresponding author. Dipartimento di Scienze e Innovazione Tecnologica (DISIT), Università del Piemonte Orientale "A. Avogadro'', Viale T. Michel 11, 15121, Alessandria (AL), Italy.
E-mail addresses: chiara.ivaldi@uniupo.it (C. Ivaldi), michele.laus@uniupo.it (M. Laus).

https://doi.org/10.1016/j.polymer.2023.126636
Received 2 October 2023; Received in revised form 12 December 2023; Accepted 26 December 2023
Available online 27 December 2023

chemistry provides great opportunities for structural reconfiguration of the polymeric material, granting various useful properties such as reprocessing, self-healing, and shape memory [5,10]. Two different rearrangement mechanisms can be distinguished for covalent adaptable networks (CANs) [10–13] (1) associative/reversible exchange (e.g., "vitrimers" [7,14]): and (2) dissociative/reversible addition (e.g., Diels-Alder systems [15]). In dissociative CANs, characterised by a discrete bond-breaking and bond-forming mechanism, the network rearrangement is inherently associated with a reduction in the number of crosslinks. As a result, these systems are more stimulus dependent and more akin to undergo undesired structural damage with respect to associative covalent adaptable networks [16]. Representative examples of dynamic chemistries in dissociative CANs include reversible cycloadditions [16–20], 1,2,3-triazolium [21] and anilinium [22] *trans*--alkylation, aza-Michael [23] and thiol-Michael reaction, and others [24,25]. In contrast, associative CANs promote network rearrangement through a bond-forming, bond-breaking single-step sequence, thus allowing the retention of crosslinking density during the dynamic exchange activation. Since the pioneering work of Leibler and co-workers [7] in 2011, many associative crosslinking chemistries for CANs have been developed, ranging from the most widely used transesterification [26–28] and transamination of vinylogous urethane [29–32], to trans (thio)esterification [33], transamination of various reactive centres [34–36], silyl ether exchange [37,38], olefin metathesis [39], dioxoborane metathesis [40], and more. Several alternatives have been proposed over years to enhance the rate of the material flow, such as the use covalently bonded catalysts [41], neighbouring group participation (NGP) to promote internal catalysis [42,43], and even catalyst free reactions [44]. Moreover, Dichel and Elling recently suggested that CANs combining dissociative and associative mechanism should be investigated to meet current industrial recycling challenges [45].

In this scenario, CANs with coexisting network rearrangement pathways have been developed, exploiting various bond exchange mechanisms at different temperatures [46], controlling the dissociation rate by modifying the chemical structure of the N-substituent [47], and associative and dissociative chemistries [48–51]. In 2021, Du Prez et al. developed dynamic covalent networks based on β-amino ester (BAE) linkages *via* aza-Michael addition of amines to acrylates, introducing the concept of reversible aza-Michael reaction in bulk polymer networks and promoting the transesterification reaction rate introducing hydroxyl groups in the β-position of the ester linkages [52]. Subsequently, Du Prez and co-workers explored the synthesis of bio-based BAEs [53] and BAE networks combined with vinylogous urethane associative chemistry [49]. Furthermore, the introduction of additional fluorine or hydroxy neighbouring groups was explored to speed up the reactivity rate of reaction [54,55]. Meanwhile Ahn and collaborators obtained shape memory and self-healing materials based on this dynamic chemistry [56]. Moreover, Engelen et al. just reported the "next-generation" BAE epoxy-based networks, based on epoxy-derived hydroxyl groups locate at the β-position of the nitrogen [57]. In the scenario of widespread use of poly(β-amino esters) (PBAEs), such as in the case of liquid crystal polymers [58] and elastomers [59–61], various studies have incorporated acrylic functionalities as network building blocks. This choice is driven by the remarkable characteristic of acrylic compounds, including high reactivity, versatility, and cost-effectiveness. Nevertheless, it is noteworthy that the use of acrylic reagents is associated with increased toxicity when compared to methacrylates, due to their lower lethal dose for 50 % of the studied population and the tendency to accumulate in aqueous media rather than fatty tissues [62,63]. Additionally, to the best of our knowledge methacrylates have not been explored for the synthesis of PBAE CANs *via* aza-Michael addition.

Within this framework, our research work has exploited the aza-Michael reaction between methacrylates and amines to synthesize catalyst-free PBAEs, with dual network exchange mechanism. Specifically, the β-amino ester moieties can undergo a catalyst-free transesterification reaction with an alcohol *via* an associative exchange reaction. In addition, the aza-Michael adducts allow for a reversible, dissociative breaking point on the electrophilic side of the dynamic unit at elevated temperatures (Scheme 1). After establishing the optimal reaction conditions for methacrylate-based networks, an industrial mixture of methacrylate monomers was used to develop an industrially relevant PBAE.

2. Experimental

2.1. Materials

Bisphenol A glycerolate (1 glycerol/phenol) diacrylate (contains 250–500 ppm MEHQ as inhibitor), 1,4-butanediol diacrylate (technical grade, contains ≈ 75 ppm of hydroquinone as inhibitor), bisphenol A glycerolate dimethacrylate, 1,4-butanediol dimethacrylate (95 %, contains 200–300 ppm MEHQ as inhibitor), and ethylene glycol dimethacrylate (98 %, 90–110 ppm monomethyl ether hydroquinone) were purchased from Sigma Aldrich (Milano, Italy). 4,4′-methylenebis (cyclohexylamine) and an industrial mixture, consisting of bisphenol A glycerolate dimethacrylate oligomers (1–3 repeating unit) and 1,4-butanediol dimethacrylate, were provided by ELANTAS Europe S.r.l. (Quattordio, Italy). Tetrahydrofuran (THF) for HPLC (≥ 99.7 %) was purchased from VWR (Milano, Italy).

2.2. Network synthesis

Acrylate-based network synthesis: a mixture of bisphenol A glycerolate diacrylate (**BPADA**) and 1,4-butanediol diacrylate (**BDA**) was prepared in 70:30 w/w, respectively, and mixed with 4,4′-methylenebis (cyclohexylamine) (**MBCA**), keeping a molar ratio of 1:0.5 between acrylate mixture to amine groups. Acrylates radical stabilizer was not removed. BPADA and MBCA were pre-heated at 70 °C to make them handleable. The mixture was poured in silicone moulds (9 cm of diameter) to reach ≈ 2 mm of thickness and heated at 70 °C for 48 h in a vacuum oven, resulting in reference A-PBAE-70 network (Scheme 2A). A transparent, solid material was obtained and prepared for characterisation.

Methacrylate-based network synthesis: a mixture of bisphenol A glycerolate dimethacrylate (**BPADM**) and 1,4-butanediol dimethacrylate (**BDM**) was prepared in 70:30 w/w, respectively, and mixed with MBCA (1 equiv. of amine to 2 equiv. of methacrylate). Methacrylate radical stabilizer was not removed. BPADM and MBCA were pre-heated at 70 °C for easy handling. The obtained mixture was poured in silicone moulds (9 cm of diameter) to reach ≈ 2 mm of thickness. Curing was performed at different temperatures (70 °C or 120 °C) and times (48 h or 15 days), resulting in different M-PBAE networks (Scheme 2B). Light yellow solid materials were obtained and prepared for characterisation.

Industrial monomer mixture-based network synthesis: a mixture of bisphenol A glycerolate dimethacrylate (**pBPADM**) oligomers (1–3 repeating unit) and BDM in 70:30 w/w respectively was supplied by ELANTAS Europe S.r.l. The average molecular weight of pBPADM oligomers, determined by ^{1}H NMR, corresponds to approximately 750 g mol^{-1}. A radical stabilizer (p-Benzochinone, 0.01 %) was solubilised in 0.5 mL of ethylene glycol dimethacrylate (EGD) and was added to the industrial mixture to inhibit radical polymerizations. MBCA was added to the mixtures (1 equiv. of amine to 2 equiv. of methacrylate). The obtained mixture was transferred in silicone moulds (9 cm of diameter) to reach ≈ 2 mm of thickness. Curing was performed at 120 °C for 15 days, resulting in I-PBAE-120 network (Scheme 3). Light orange solid materials were obtained and prepared for characterisation.

2.3. Characterization

Fourier Transformed Infrared (FTIR) spectroscopy was performed using a Nicolet iN10 (Thermo Scientific) equipped with iZ10, equipped with DTGS detector. The analysis was performed in transmission mode in a

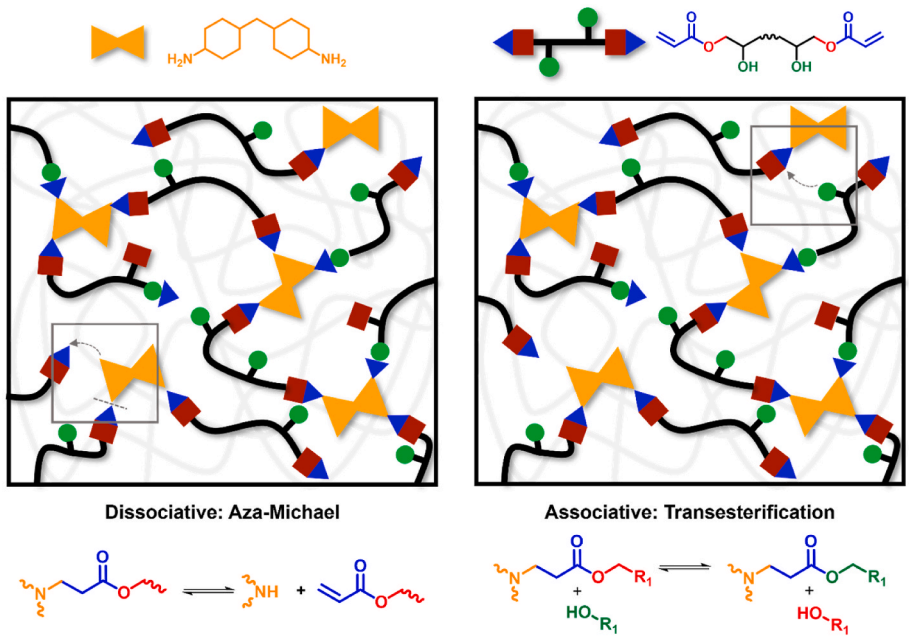

Scheme 1. Display of dual network rearrangement via dissociative retro aza-Michael reaction and associative transesterification.

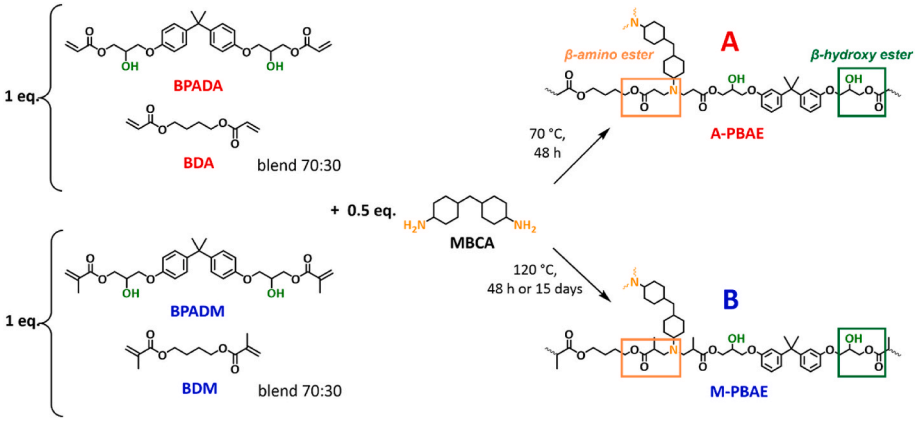

Scheme 2. Schematic representation of the synthesis of A-PBAE and M-PBAE networks starting from BPADA/BDA or BPADM/BDM monomer mixtures and MBCA as crosslinker. Catalysis by neighbouring group participation effect is granted by β-amino and β-hydroxyalkyl moieties.

wavenumber range of 4000–400 cm^{-1}. The instrument was controlled by OMNIC™ Picta software. A total number of 64 scans were acquired for each spectrum, with a spectral resolution of 4 cm^{-1}. Industrial sample after mould reprocessing (RI-PBAE-120) and after water contact (H_2OI-PBAE-120) were diluted with KBr and analysed as pellets. Spectra were normalized with respect to the pellet weight. For kinetics experiments, an aliquot of sample was deposited on a KBr solid support and analysed without further manipulations, focusing on the same sample area. FT-IR conversion was determined after deconvolution by quantifying the area of the signal at 810 cm^{-1}. To ensure comparability among the spectra areas, the area of the signal at 810 cm^{-1} (A_{814}) of each spectrum was normalized to the area of the corresponding signal at 830 cm^{-1}(A_{830}), which remained constant over time. The conversion was calculated according to eq. (1):

$$C = \frac{R_i - R_t}{R_i}\ 100 \qquad (1)$$

with $R_i = A_{810,0h}/A_{830,0h}$ and $R_t = A_{810,t}/A_{830,t}$.

Differential scanning calorimetry (DSC) analyses were performed using a Mettler-Toledo Calorimetry mod. 821^e instrument on 10 mg of sample in alumina sealed crucibles. The glass transition temperature (T_g) was determined with a two-runs program. The sample was heated under nitrogen atmosphere from −60 °C to 120 °C at a heating rate of 20 °C/min, cooled till −60 °C at 10 °C/min and heated again up to 300 °C at 20 °C/min.

Rheology experiments were performed using an strain-controlled rheometer mod. ARES (Rheometric Scientific) equipped with parallel plate geometry using 25 mm sample disk, with thickness of ≈ 2 mm. The experiments were performed at different temperatures (120, 140, 160 and 180 °C), applying a strain of 1.0 % and using a normal force of 1 N for I-PBAE-120 and A-PBAE-70, and 5 N for M-PBAE-120. The relaxation storage modulus $G(t)$ was followed as a function of time at constant temperature. From this dataset the characteristic relaxation time τ^* was estimated. According to the Maxwell's model for viscoelastic liquids, the relaxation time τ^* at a certain temperature is considered equal to the time required for the relaxation modulus $G(t)$ to reach 37 % of its starting value G_0, namely (eq. (2)):

$$\frac{G(t)}{G_0} = \frac{1}{e} \qquad (2)$$

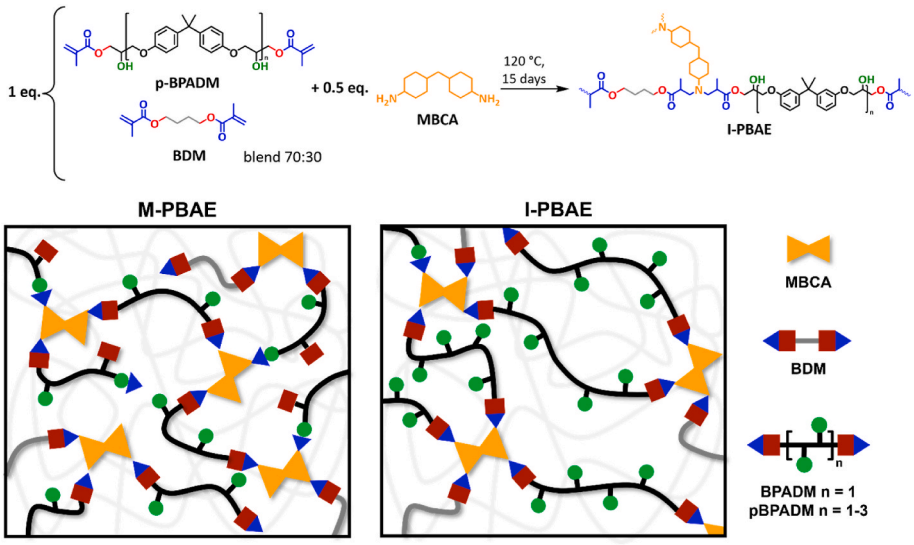

Scheme 3. Representation of I-PBAE-120 synthesis (top) and schematic comparison of M-PBAE and I-PBAE networks (bottom), specifically regarding number of hydroxyl moieties and crosslinking density.

Then, an Arrhenius-type law (eq. (3)) was employed to describe the evolution of τ * as a function of temperature as the network relaxation evolves as a consequence of the exchange reactions:

$$\tau^* = \tau \bullet e^{\frac{E_a}{RT}} \tag{3}$$

where τ is a pre-exponential factor and E_a is the flow activation energy.

Thermogravimetric analyses (TGA) were performed using a Mettler-Toledo TGA/SDC 3+ under nitrogen flow (carrier gas flow rate 50 mL/min), from 25 to 900 °C at a heating rate of 10 °C/min.

2.4. Solubility and hydrolysis tests

The *soluble fraction* of the crosslinked materials was evaluated through immersion in a good solvent for the monomers. Approximatively 100 mg of the samples were put in contact with 5 mL of tetrahydrofuran (THF) for 7 days at room temperature. Upon solvent removal, the samples were dried under vacuum for 24 h at 50 °C. The soluble fraction was estimated using eq. (4):

$$soluble\ fraction\ (\%) = 100 \bullet \frac{m_i - m_d}{m_i} \tag{4}$$

Where m_i represents the initial mass, and m_d the dry mass.

Hydrolysis tests were performed on I-PBAE-120 by immersing around 100 mg of samples in 5 mL of demineralised water for 7 days at room temperature, drying samples in an oven for 24 h and determining the soluble fraction according to eq. (4). The glass transition temperature (T_g) of the material was monitored during the water contact by means of DSC analysis. At the end of the hydrolysis test, recovered material was heated at 100 °C under vacuum for 24 h and the T_g was again determined.

2.5. Shape memory and reprocessability

Remoulding ability through thermoforming and shape recovery was tested on specimens with dimensions of (25 mm × 4 mm × 2.5 mm). Flat rectangular panels were first equilibrated in an oven at 160 °C (T > T_g) for 10 min, after which they were manually moulded into various shapes using tweezers. The reshaped samples were then gradually cooled to 25 °C (T < T_g) while maintaining the applied force. Subsequently, the applied stress was released to fix the temporary shape. Finally, the samples were reheated to 160 °C to initiate shape recovery. This entire process was repeated several times.

To reprocess the network, 10 g of the polymer were broken into pieces and placed into a mould (40 mm × 40 mm x 5 mm) for compression moulding. The sample was then inserted into a preheated hydraulic press at 160 °C for 30 min under a pressure of 3 tons. Subsequently, the reprocessed material was cooled to room temperature and carefully removed from the mould.

3. Results and discussion

3.1. Comparative kinetics of Aza-Michael addition reactions in acrylate and methacrylate-based CANs

Kinetic studies were performed to establish the best reaction conditions in terms of time and temperature to synthesize methacrylate-based covalent adaptable networks characterised by crosslinking densities comparable to similar acrylate-based CANs reported in literature [52, 56]. One of the difficulties in handling acrylic long-chain monomers is their high viscosity, so it is necessary to preheat the reactants before the reaction. At industrial level, these monomers are mixed with other low molecular weight reactants that serve as solvent, leading to lower viscosities and thus making the reaction mixture more manageable in the manufacturing process. Due to the necessity of developing an industrial product, in this research work β-amino ester-based networks were synthesised *via* aza-Michael addition of 4,4′-methylenebis(cyclohexylamine) (MBCA) with a mixture of bisphenol A glycerolate diacrylate (BPADA) and butanediol diacrylate (BDA), or bisphenol A glycerolate dimetacrylate (BPADM) and butanediol dimethacrylate (BDM), respectively (Scheme 2), using a scalable one-step procedure, to obtain A-PBAE or M-PBAE covalent adaptable networks. BDA/BDM monomers were added to lower the viscosity of BPADA/BPADM long-chain bisphenol-based reactants.

Since network topology, number of crosslinks, and material flow are clearly affected by stoichiometry, an amine-to-methacrylate/acrylate equivalent ratio of 0.5:1 was chosen. This ratio ensures that, in principle, every primary and secondary amine can react with an acrylic functionality, leading to a perfect network structure. For deviation from this value to either side, the cross-linking density will be reduced [57].

The aza-Michael addition was performed at 70 °C for the acrylate-based CAN (A-PBAE-70). The choice of temperature was based on established literature procedure that had been developed for a similar reaction involving the BPADA monomer [52]. The reaction conversion,

which corresponds to an increase of the crosslinking density, was monitored by determining the evolution of the glass transition temperature (T_g) as a function of time for both acrylate-based and methacrylate-based reactions. After 48 h, A-PBAE-70 was characterised by a glass transition temperature of 42 °C, as measured by differential scanning calorimetry (DSC) (Fig. 1A). It is important to highlight that this T_g value is comparable to what reported in literature for CANs synthesised in similar conditions in absence of low molecular weight reactants [52,55]. This experimental result suggests that the use of BDA in addition to BPADA do not compromise the thermal properties of the final network. Under identical experimental conditions, the methacrylate-based material (M-PBAE-70) resulted in a T_g value of 25 °C. This value is notably lower than the one obtained for A-PBAE-70. As expected, methacrylates are less reactive in Michael addition than acrylates, primarily due to steric hindrance and inductive effect of methyl group bound to the α carbon [64,65]. Consequently, M-PBAE-70 was not further characterised. To speed up the reaction rate, the curing temperature of the M-PBAE was raised to 120 °C, resulting in a material with a glass transition temperature of 48 °C after 48 h, and characterised by a crosslinking density comparable to that of A-PBAE-70.

To assess the effectiveness of the crosslinking reaction, solubility tests were performed. No soluble fraction was detected for A-PBAE-70, confirming excellent solvent resistance attributed to the high crosslinking density of the dynamic network. In contrast, M-PBAE-120 still exhibit a residual soluble fraction (11 %, Table 1) after 48 h of reaction. Extending the reaction time to 15 days facilitated further increase in the crosslinking density, leading to a solubility of approximately 2 %.

Network formation was qualitatively verified by means of FT-IR spectroscopy (Fig. 1B). A steady reduction in the aliphatic C═C stretching mode band (1636 cm^{-1}) of acrylate/methacrylates monomers was detected as the aza-Michael addition progresses over time. Accordingly, signals ascribable to in plane scissoring of = CH_2 vinyl groups (1410 cm^{-1}), and out of plane bending of = C–H groups (810 cm^{-1}) significantly decreased, together with N–H stretching modes at 3430 cm^{-1} and 3300 cm^{-1} related to MBCA amine, thus indicating the successful formation of crosslinks. Simultaneously, the broad band at 3350 cm^{-1} due to the O–H stretching mode of hydroxyl groups became more pronounced with increasing BPADA/BPADM content in the PBAEs network, as well as typical shift of 10 cm^{-1} of the C═O signal from 1734/1726 cm^{-1} to 1724/1716 cm^{-1} for A-PBAE-70/M-PBAE-120 was detected, indicating successful incorporation of vinylic monomers during the formation of PBAEs architectures (monomer spectra reported in Fig. S1).

3.2. Industrial methacrylate-based CAN: synthesis and hydrolysis tests

After establishing the best synthesis conditions for methacrylate-based PBAEs, an industrial mixture of bisphenol A glycerolate dimethacrylate-based oligomers (referred as pBPADM) and 1,4-butanediol dimethacrylate (BDM) (FT-IR spectra reported in Fig. S2) was used in combination with MBCA to obtain an industrial monomer-based covalent adaptable network (I-PBAE). In this study, an amine-to-methacrylate molar ratio of 0.5:1 was selected, and reaction temperature was set to 120 °C based on previous data. With respect to M-PBAE-120, the as-obtained I-PBAE-120 exhibit differences in the number of bisphenol A glycerolate repeating units in the polymer chains (n = 1–3). As a result, the number of hydroxyl groups responsible for stimulating internal catalysis *via* neighbouring group participation (NPG) effect is significantly enhanced. Additionally, due to the longer monomer length of pBPADM, the crosslinking density is lower than that of the model analogue (Scheme 3).

Table 1
Characterisation of PBAE-based networks.

CAN	Acrylates mixture	$T_{gDSC-48h}$ [°C][a]	$T_{gDSC-15d}$ [°C][a]	SF_{-48h} [%][b]	SF_{-15d} [%][b]
A-PBAE-70	BPADA + BDA	42	–	[c]	–
M-PBAE-120	BPADM + BDM	48	75	11	2

[a] DSC glass transition temperature (T_{gDSC}) measured after 48 h and 15 days.
[b] SF = soluble fraction obtained after sample immersion in THF for 7 days at rt.
[c] No soluble fraction detected.

The aza-Michael reaction was monitored by estimating the evolution of glass transition temperature over time. As the addition reaction proceeded, an increment in the glass transition temperature value was detected, indicating progressive increase in the crosslinking density of the dynamic network (Fig. 2A). After 15 days, the T_g value was found to be comparable with the one recorded for M-PBAE-120 network. Solvent resistance was determined by performing solubility tests, resulting in a soluble fraction of 6 % at the end of the curing process (Table 2). Moreover, the degree of conversion was estimated by means of FT-IR analysis (Fig. 2B), by quantifying the area of the signal at 810 cm^{-1} ascribable to the out of plane C–H bending of the alkene. The conversion value at each reaction time, together with the areas of the IR bands, are reported in Table S1 and Fig. S3, respectively. After 15 days of reaction, a double bonds conversion of approximately 60 % has been achieved. Moreover, considerations regarding competitive side reactions, such as radical homopolymerization and amidation, were taken into account. Specifically, after exposing the methacrylate mixture to the identical curing conditions applied to I-PBAE-120, the retention of the aliphatic C═C stretching mode at 1636 cm^{-1} and of the out of plane C–H bending at 810 cm^{-1} indicates the radical stabilizer's efficacy to impede radical

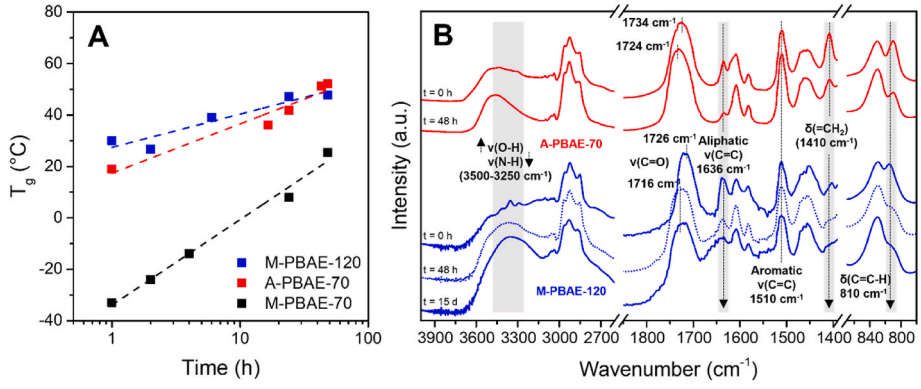

Fig. 1. A) Evolution of glass transition temperature as a function of time (1–48 h) for A-PBAE-70 (red curve), M-PBAE-70 (black curve) and M-PBAE-120 (blue curve). B) FTIR-spectra of A-PBA-E 70 (red curves) and M-PBAE-120 (blue curves) CANs. A comparison between initial time reaction (0 h) and end of the curing (48 h or 15 d) is reported. (For interpretation of the references to colour in this figure legend, the reader is referred to the Web version of this article.)

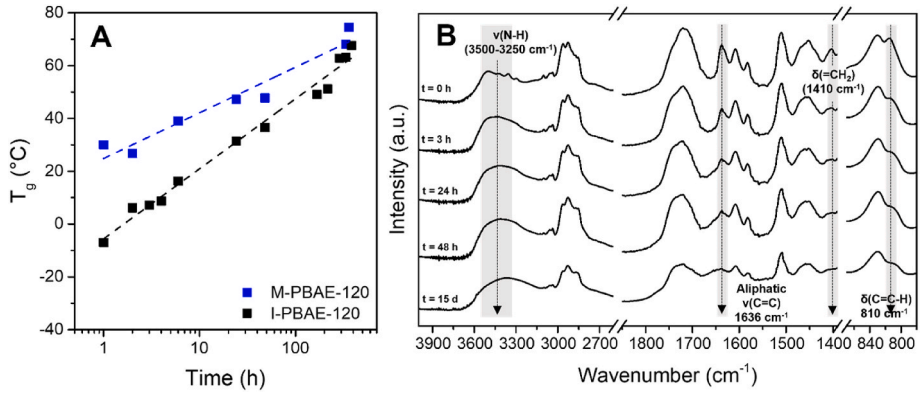

Fig. 2. A) Evolution of glass transition temperature as a function of time (1 h-15days) for M-PBAE-120 (blue curve) and I-PBAE-120 (black curve). B) Aza-Michael reaction between p-BPADM and BDM mixture and MBCA followed by FT-IR spectroscopy over time. (For interpretation of the references to colour in this figure legend, the reader is referred to the Web version of this article.)

Table 2
Thermal and soluble properties of I-PBAE-120.

CAN	Acrylates mixture	[a]$T_{gDSC\text{-}48h}$ [°C]	[a]$T_{gDSC\text{-}15d}$ [°C]	[b]$T_{gDSC\text{-}wc}$ [°C]	[c]$T_{gDSC\text{-}out}$ [°C]	[d]$SF_{\text{-}15d}$ [%]	[e]$C_{\text{-}15d}$ [%]
I-PBAE-120	pBPADM + BDM	37	68	28	68	6	57.51

[a] DSC glass transition temperature measured after 48 h and 15 days.
[b] DSC T_g after 30 days water contact.
[c] DSC T_g after outgassing sample at 100 °C overnight, after water contact.
[d] SF = soluble fraction obtained after sample immersion in THF for 7 days at rt.
[e] Conversion of methacrylate groups evaluated after deconvolution of IR signal at 810 cm^{-1}.

homopolymerization (Fig. S4A). Additionally, an I-PBAE-120-1% network was synthesised by adding to the methacrylate mixture a higher inhibitor content (1 % w/w) and its glass transition temperature was monitored over time. Despite the significant increase in the radical stabilizer concentration, no significant variation in the T_g values was observed (Fig. S4B). Furthermore, the lack of strong and intense bands associated with amide formation, notably amide I band between 1700 and 1650 cm^{-1} and amide II between 1650 and 1520 cm^{-1}, confirmed the non-occurrence of amidation reaction during the synthesis of I-PBAE-120 network (Fig. S5).

To evaluate the hydrolysis resistance of I-PBAE-120, water contact tests were performed. To that end, glass transition temperature was monitored over time, resulting in a decrease from 68 °C to 28 °C after 30 days of immersion in water (Fig. 3A). The retention of chemical composition of the network upon hydrolysis testing was confirmed by means of FT-IR analysis (Fig. 3B). Notably, no bands associated to degradation products were detected in the spectrum of H_2O–I-PBAE-120 when compared to the pristine material. These findings strongly indicate that water acts as a plasticizer, expanding the available free volume within the polymer matrix and reducing intermolecular forces. Due to the increased mobility among polymer chain, the glass transition temperature decreases over time. To further support this hypothesis, H_2O–I-PBAE-120 was outgassed at 100 °C for 24 h to remove water and initial T_g value was fully recovered (Table 2).

3.3. Dynamic properties of I-PBAE network

The dynamic behaviour of the I-PBAE-120 network, was assessed by means of rheological analysis. Stress relaxation (SR) experiments were performed monitoring the response of the material in terms of relaxation modulus $G(t)$ as a function of time at different temperatures. The network displayed relaxation of applied stress in the investigated temperature range (from 120 to 180 °C), demonstrating typical viscoelastic fluid behaviour and indicating the presence of exchangeable linkages

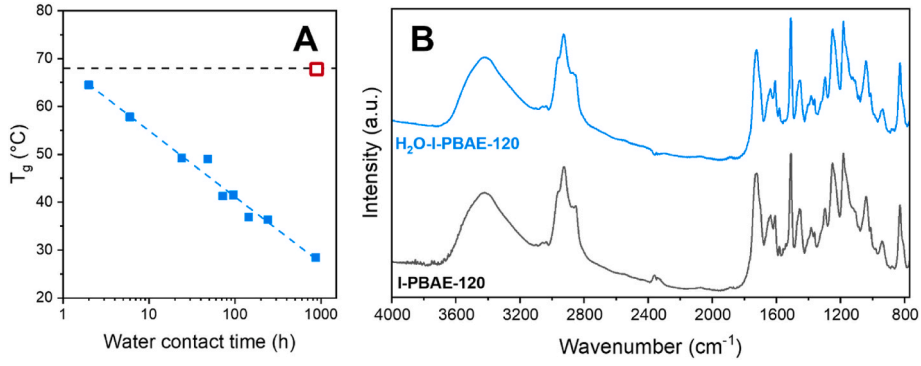

Fig. 3. A) Glass transition temperature as a function of water contact time for H_2O–I-PBAE-120 sample (light blue filled squares) and recovered T_g value after heating and outgassing the sample (hollow red square). Black dashed line corresponds to the T_g value of the pristine sample. B) FT-IR of H_2O–I-PBAE-120 (light blue) compared to pristine I-PBAE-120 (black curve). (For interpretation of the references to colour in this figure legend, the reader is referred to the Web version of this article.)

within the macromolecular architecture. To quantify the extent of this rearrangement, Maxwell model of single exponential decay was employed to fit the data [66] (Fig. 4A, refer to Fig. S6 for normalized SR curves and to Fig. S7 for not normalized SR curves) and to determine the characteristic relaxation time at $1/e$ (τ^*) at each temperature. Based on the relaxation curves reported in Fig. 4A, τ^* values for I-PBAE-120 range from 51 s to 55 min, at 180 and 120 °C respectively (Table S2). A flow activation energy $E_{a(flow)}$ of 134 kJ/mol was calculated using Arrhenius law dependence of τ^* on temperature (eq. (3), Fig. S8).

To get a deeper insight in the network rearrangement mechanism, comparative stress relaxation experiments of A-PBAE-70, M-PBAE-120, and I-PBAE-120 at 160 °C were performed (Fig. 4B). It is noteworthy that exchange rate of all the networks is increased by a double neighbouring group participation (NGP) effect, with β-amino functionality and β-hydroxyalkyl moieties activating the electrophilic or the nucleophilic side of the ester group respectively (Scheme 2). Additionally, it has been reported that BPAEs with β-hydroxyl groups relaxed approximately 15–20 times faster than the non-hydroxylated CANs at 160 °C [56]. Indeed, each of the networks exhibited stress relaxation at 160 °C. Specifically, the fastest exchange rate was observed for A-BPAE-70. In contrast, steric hindrance and inductive effect of methyl group bound to the α-carbon drastically slowed down the network relaxation of M-PBAE-120 when compared to the acrylate-based analogue. Notably, I-PBAE-120 displayed a faster dynamic covalent exchange with respect to M-PBAE-120. This behaviour can be attributed to the increased number of pendent hydroxyl groups in bisphenol A building blocks and a reduced crosslinking density resulting from the longer average length of bis-methacrylate moiety. In contrast, the slower relaxation rate observed for I-PBAE-120 in comparison to A-PBAE-70 can be ascribed to the inherently lower reactivity of methacrylates with respect to their acrylate counterparts. This concept has been already discussed in the model study section and it is well-established within scientific literature [63].

3.4. Shape memory and reprocessability of I-PBAE network

After investigating the thermal and dynamic properties of model CANs and those obtained using the industrial monomers, I-PBAE-120 was selected as a representative sample to showcase its shape memory capabilities and reprocessing upon appropriate thermo-mechanical stimulation. As depicted in Fig. 5A, the sample was heated at 160 °C to enable shape modification. Then, after the cooling step, the polymer transitions into a rigid state, effectively 'locking in' the shape. When exposed to heat once more, it softens and gradually returns to its original shape. This shape memory behaviour confirms that the material underwent complete stress relaxation due to its vitrimeric characteristics. Finally, the mechanical recycling was demonstrated through hot pressing. 10 g of I-PBAE-120 were grinded in a ball mill and loaded into a steel mould for compression. A pressure of 3 tons was applied for 30 min at 160 °C, followed by cooling to room temperature. Thanks to successful granule sintering and favourable thermo-mechanically induced vitrimeric material viscous flow, RI-PBAE-120 material could be recovered as a single piece with a well-defined shape and no macroscopic defects (Fig. 5B). After reprocessing, glass transition temperature of RI-PBAE-120 was comparable with the pristine sample value (Table S2). Moreover, thermal analyses and FT-IR spectra assessed the retention of chemical composition and material properties over recycling (Figs. S10 and S11, Table S3).

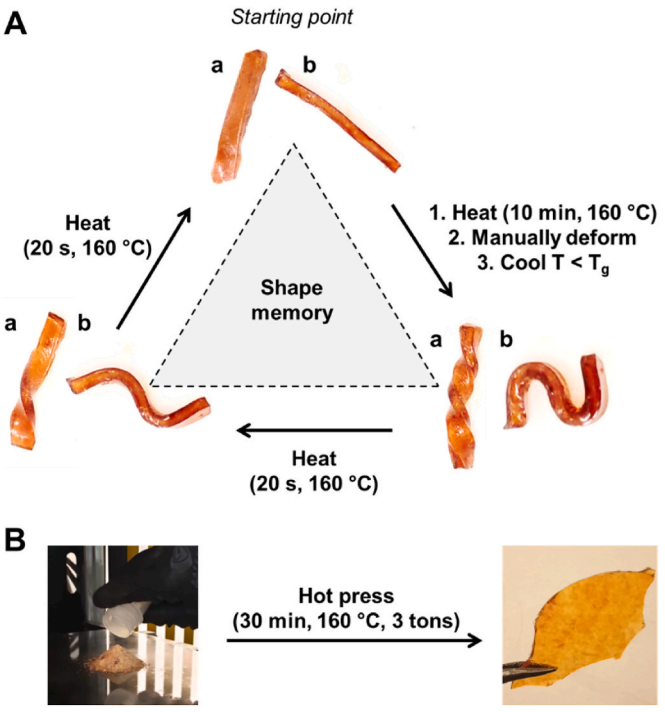

Fig. 5. Demonstration of (A) reusability *via* thermoforming reprocessing and (B) recycling *via* hot pressing at 3 tons. For both processes, temperature was set at 160 °C.

4. Conclusions

In this research study, the suitability of methacrylate monomers for vitrimer synthesis has been demonstrated, suggesting their potential in

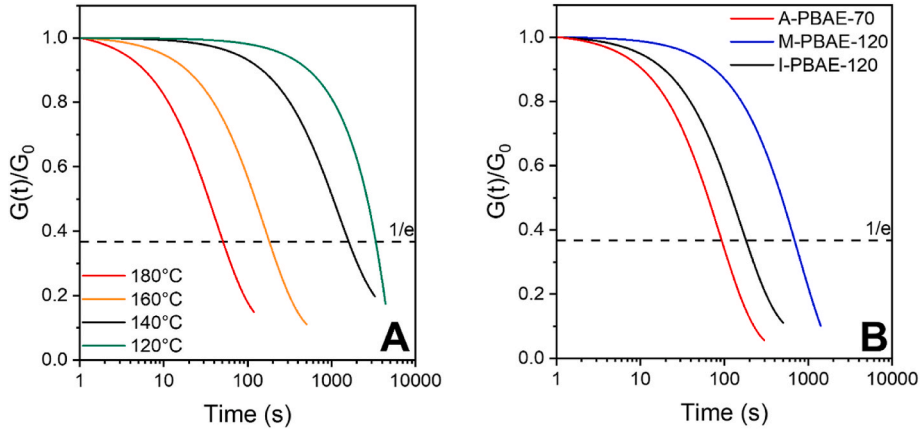

Fig. 4. A) Normalized stress relaxation curves of I-PBAE-120 from 120 to 180 °C and B) and stress relaxation comparison of elastomeric dynamic PBAEs at 160 °C. All the reported curves were fit with Maxwell model of single exponential decay.

providing electron-deficient alkenes for the aza-Michael addition reaction. Nevertheless, the synthetic conditions in terms of reaction time and temperature are much more demanding for the network prepared using methacrylate monomers compared to acrylic monomers. Despite these limitations, an industrial methacrylate-based PBAE network has been successfully developed as an alternative to conventional non-recyclable thermosets. The dynamicity of this CAN was enabled by a combination of dissociative reversible aza-Michael addition and associative trans-esterification reaction, acting synergically at different side of the electrophilic centre of the ester group, and further speeded up by increased number of hydroxyl groups with respect to the model analogue. Indeed, upon rheological stress relaxation test, the industrial methacrylate-based network demonstrated the ability to relax the applied stress at different temperatures, with an activation energy in good coherence with previous reported PBAEs. Moreover, on the basis of the dynamic features, this elastomer successfully demonstrated shape memory and shape reconfiguration properties, as well as reprocessing of upon mild thermo-mechanical treatments (160 °C, 30 min), while retaining its chemical structure.

CRediT authorship contribution statement

Chiara Ivaldi: Writing – original draft, Writing – review & editing. **Erica Laguzzi:** Data curation, Formal analysis, Investigation. **Viviana Maria Ospina:** Data curation, Investigation, Visualization, Writing – original draft. **Diego Antonioli:** Data curation, Formal analysis. **Riccardo Chiarcos:** Writing – review & editing. **Federica Campo:** Project administration, Validation. **Nicola Cuminetti:** Validation. **Janosc De Buck:** Validation. **Michele Laus:** Methodology, Supervision, Validation.

Declaration of competing interest

The authors declare the following financial interests/personal relationships which may be considered as potential competing interests: Michele Laus reports financial support was provided by ELANTAS Europe Srl.

Data availability

Data will be made available on request.

Acknowledgements

This work was financially supported by ELANTAS Europe S.r.l. (Quattordio, Italy).

Appendix A. Supplementary data

Supplementary data to this article can be found online at https://doi.org/10.1016/j.polymer.2023.126636.

References

[1] J.-G. Rosenboom, R. Langer, G. Traverso, Bioplastics for a circular economy, Nat. Rev. Mater. 7 (2022) 117–137, https://doi.org/10.1038/s41578-021-00407-8.
[2] Y. Zhu, C. Romain, C.K. Williams, Sustainable polymers from renewable resources, Nature 540 (2016) 354–362, https://doi.org/10.1038/nature21001.
[3] OECD, Global Plastics Outlook, Policy Scenarios to 2060, OECD, 2022, https://doi.org/10.1787/aa1edf33-en.
[4] J.F. Patrick, M.J. Robb, N.R. Sottos, J.S. Moore, S.R. White, Polymers with autonomous life-cycle control, Nature 540 (2016) 363–370, https://doi.org/10.1038/nature21002.
[5] J. Zheng, Z.M. Png, S.H. Ng, G.X. Tham, E. Ye, S.S. Goh, X.J. Loh, Z. Li, Vitrimers: current research trends and their emerging applications, Mater. Today 51 (2021) 586–625, https://doi.org/10.1016/j.mattod.2021.07.003.
[6] L. Imbernon, S. Norvez, From landfilling to vitrimer chemistry in rubber life cycle, Eur. Polym. J. 82 (2016) 347–376, https://doi.org/10.1016/j.eurpolymj.2016.03.016.
[7] D. Montarnal, M. Capelot, F. Tournilhac, L. Leibler, Silica-Like malleable materials from permanent organic networks, Science 334 (2011) 965–968, https://doi.org/10.1126/science.1212648.
[8] T.F. Scott, A.D. Schneider, W.D. Cook, C.N. Bowman, Photoinduced plasticity in cross-linked polymers, Science 308 (2005) 1615–1617, https://doi.org/10.1126/science.1110505.
[9] J.L. Self, N.D. Dolinski, M.S. Zayas, J. Read De Alaniz, C.M. Bates, Brønsted-acid-catalyzed exchange in polyester dynamic covalent networks, ACS Macro Lett. 7 (2018) 817–821, https://doi.org/10.1021/acsmacrolett.8b00370.
[10] J.M. Winne, L. Leibler, F.E. Du Prez, Dynamic covalent chemistry in polymer networks: a mechanistic perspective, Polym. Chem. 10 (2019) 6091–6108, https://doi.org/10.1039/C9PY01260E.
[11] C.J. Kloxin, C.N. Bowman, Covalent adaptable networks: smart, reconfigurable and responsive network systems, Chem. Soc. Rev. 42 (2013) 7161–7173, https://doi.org/10.1039/C3CS60046G.
[12] M. Podgórski, B.D. Fairbanks, B.E. Kirkpatrick, M. McBride, A. Martinez, A. Dobson, N.J. Bongiardina, C.N. Bowman, Toward stimuli-responsive dynamic thermosets through continuous development and improvements in covalent adaptable networks (CANs), Adv. Mater. 32 (2020) 1906876, https://doi.org/10.1002/adma.201906876.
[13] G.M. Scheutz, J.J. Lessard, M.B. Sims, B.S. Sumerlin, Adaptable crosslinks in polymeric materials: resolving the intersection of thermoplastics and thermosets, J. Am. Chem. Soc. 141 (2019) 16181–16196, https://doi.org/10.1021/jacs.9b07922.
[14] W. Denissen, J.M. Winne, F.E. Du Prez, Vitrimers: permanent organic networks with glass-like fluidity, Chem. Sci. 7 (2016) 30–38, https://doi.org/10.1039/C5SC02223A.
[15] X. Chen, M.A. Dam, K. Ono, A. Mal, H. Shen, S.R. Nutt, K. Sheran, F. Wudl, A thermally Re-mendable cross-linked polymeric material, Science 295 (2002) 1698–1702, https://doi.org/10.1126/science.1065879.
[16] K.K. Oehlenschlaeger, J.O. Mueller, J. Brandt, S. Hilf, A. Lederer, M. Wilhelm, R. Graf, M.L. Coote, F.G. Schmidt, C. Barner-Kowollik, Adaptable hetero diels-alder networks for fast self-healing under mild conditions, Adv. Mater. 26 (2014) 3561–3566, https://doi.org/10.1002/adma.201306258.
[17] B.J. Adzima, H.A. Aguirre, C.J. Kloxin, T.F. Scott, C.N. Bowman, Rheological and chemical analysis of reverse gelation in a covalently cross-linked Diels−Alder polymer network, Macromolecules 41 (2008) 9112–9117, https://doi.org/10.1021/ma801863d.
[18] C. Chapelle, B. Quienne, C. Bonneaud, G. David, S. Caillol, Diels-Alder-Chitosan based dissociative covalent adaptable networks, Carbohydr. Polym. 253 (2021) 117222, https://doi.org/10.1016/j.carbpol.2020.117222.
[19] P. Reutenauer, E. Buhler, P.J. Boul, S.J. Candau, J.-M. Lehn, Room temperature dynamic polymers based on diels-alder chemistry, Chem. Eur J. 15 (2009) 1893–1900, https://doi.org/10.1002/chem.200802145.
[20] S.D. Bergman, F. Wudl, Mendable polymers, J. Mater. Chem. 18 (2008) 41–62, https://doi.org/10.1039/B713953P.
[21] M.M. Obadia, A. Jourdain, P. Cassagnau, D. Montarnal, E. Drockenmuller, Tuning the viscosity profile of ionic vitrimers incorporating 1,2,3-triazolium cross-links, Adv. Funct. Mater. 27 (2017) 1703258, https://doi.org/10.1002/adfm.201703258.
[22] P. Chakma, Z.A. Digby, M.P. Shulman, L.R. Kuhn, C.N. Morley, J.L. Sparks, D. Konkolewicz, Anilinium salts in polymer networks for materials with mechanical stability and mild thermally induced dynamic properties, ACS Macro Lett. 8 (2019) 95–100, https://doi.org/10.1021/acsmacrolett.8b00819.
[23] R. Baruah, A. Kumar, R.R. Ujjwal, S. Kedia, A. Ranjan, U. Ojha, Recyclable thermosets based on dynamic amidation and aza-michael addition chemistry, Macromolecules 49 (2016) 7814–7824, https://doi.org/10.1021/acs.macromol.6b01807.
[24] H. Liu, A.Z. Nelson, Y. Ren, K. Yang, R.H. Ewoldt, J.S. Moore, Dynamic remodeling of covalent networks via ring-opening metathesis polymerization, ACS Macro Lett. 7 (2018) 933–937, https://doi.org/10.1021/acsmacrolett.8b00422.
[25] K. Jin, L. Li, J.M. Torkelson, Recyclable crosslinked polymer networks via one-step controlled radical polymerization, Adv. Mater. 28 (2016) 6746–6750, https://doi.org/10.1002/adma.201600871.
[26] E. Manarin, F. Da Via, B. Rigatelli, S. Turri, G. Griffini, Bio-based vitrimers from 2,5-furandicarboxylic acid as repairable, reusable, and recyclable epoxy systems, ACS Appl. Polym. Mater. 5 (2023) 828–838, https://doi.org/10.1021/acsapm.2c01774.
[27] M. Capelot, D. Montarnal, F. Tournilhac, L. Leibler, Metal-catalyzed transesterification for healing and assembling of thermosets, J. Am. Chem. Soc. 134 (2012) 7664–7667, https://doi.org/10.1021/ja302894k.
[28] R.L. Snyder, D.J. Fortman, G.X. De Hoe, M.A. Hillmyer, W.R. Dichtel, Reprocessable acid-degradable polycarbonate vitrimers, Macromolecules 51 (2018) 389–397, https://doi.org/10.1021/acs.macromol.7b02299.
[29] J.J. Lessard, L.F. Garcia, C.P. Easterling, M.B. Sims, K.C. Bentz, S. Arencibia, D. A. Savin, B.S. Sumerlin, Catalyst-free vitrimers from vinyl polymers, Macromolecules 52 (2019) 2105–2111, https://doi.org/10.1021/acs.macromol.8b02477.
[30] W. Denissen, G. Rivero, R. Nicolaÿ, L. Leibler, J.M. Winne, F.E. Du Prez, Vinylogous urethane vitrimers, Adv. Funct. Mater. 25 (2015) 2451–2457, https://doi.org/10.1002/adfm.201404553.
[31] W. Denissen, M. Droesbeke, R. Nicolaÿ, L. Leibler, J.M. Winne, F.E. Du Prez, Chemical control of the viscoelastic properties of vinylogous urethane vitrimers, Nat. Commun. 8 (2017) 14857, https://doi.org/10.1038/ncomms14857.
[32] Y. Amamoto, H. Otsuka, A. Takahara, K. Matyjaszewski, Self-healing of covalently cross-linked polymers by reshuffling thiuram disulfide moieties in air under visible

light, Adv. Mater. 24 (2012) 3975–3980, https://doi.org/10.1002/adma.201201928.
[33] C. Wang, T.M. Goldman, B.T. Worrell, M.K. McBride, M.D. Alim, C.N. Bowman, Recyclable and repolymerizable thiol–X photopolymers, Mater. Horiz. 5 (2018) 1042–1046, https://doi.org/10.1039/C8MH00724A.
[34] C. Taplan, M. Guerre, C.N. Bowman, F.E. Du Prez, Surface modification of (Non)-Fluorinated vitrimers through dynamic transamination, Macromol. Rapid Commun. 42 (2021) 2000644, https://doi.org/10.1002/marc.202000644.
[35] P. Taynton, H. Ni, C. Zhu, K. Yu, S. Loob, Y. Jin, H.J. Qi, W. Zhang, Repairable woven carbon fiber composites with full recyclability enabled by malleable polyimine networks, Adv. Mater. 28 (2016) 2904–2909, https://doi.org/10.1002/adma.201505245.
[36] C. Taplan, M. Guerre, J.M. Winne, F.E. Du Prez, Fast processing of highly crosslinked, low-viscosity vitrimers, Mater. Horiz. 7 (2020) 104–110, https://doi.org/10.1039/C9MH01062A.
[37] Y. Nishimura, J. Chung, H. Muradyan, Z. Guan, Silyl ether as a robust and thermally stable dynamic covalent motif for malleable polymer design, J. Am. Chem. Soc. 139 (2017) 14881–14884, https://doi.org/10.1021/jacs.7b08826.
[38] P. Zheng, T.J. McCarthy, A surprise from 1954: siloxane equilibration is a simple, robust, and obvious polymer self-healing mechanism, J. Am. Chem. Soc. 134 (2012) 2024–2027, https://doi.org/10.1021/ja2113257.
[39] Y.-X. Lu, Z. Guan, Olefin metathesis for effective polymer healing via dynamic exchange of strong carbon–carbon double bonds, J. Am. Chem. Soc. 134 (2012) 14226–14231, https://doi.org/10.1021/ja306287s.
[40] M. Röttger, T. Domenech, R. Van Der Weegen, A. Breuillac, R. Nicolaÿ, L. Leibler, High-performance vitrimers from commodity thermoplastics through dioxaborolane metathesis, Science 356 (2017) 62–65, https://doi.org/10.1126/science.aah5281.
[41] Y. Yang, E.M. Terentjev, Y. Wei, Y. Ji, Solvent-assisted programming of flat polymer sheets into reconfigurable and self-healing 3D structures, Nat. Commun. 9 (2018) 1906, https://doi.org/10.1038/s41467-018-04257-x.
[42] F. Cuminet, S. Caillol, É. Dantras, É. Leclerc, V. Ladmiral, Neighboring group participation and internal catalysis effects on exchangeable covalent bonds: application to the thriving field of vitrimer chemistry, Macromolecules 54 (2021) 3927–3961, https://doi.org/10.1021/acs.macromol.0c02706.
[43] M. Guerre, C. Taplan, J.M. Winne, F.E. Du Prez, Vitrimers: directing chemical reactivity to control material properties, Chem. Sci. 11 (2020) 4855–4870, https://doi.org/10.1039/D0SC01069C.
[44] S. Debnath, S. Kaushal, U. Ojha, Catalyst-free partially bio-based polyester vitrimers, ACS Appl. Polym. Mater. 2 (2020) 1006–1013, https://doi.org/10.1021/acsapm.0c00016.
[45] B.R. Elling, W.R. Dichtel, Reprocessable cross-linked polymer networks: are associative exchange mechanisms desirable? ACS Cent. Sci. 6 (2020) 1488–1496, https://doi.org/10.1021/acscentsci.0c00567.
[46] M. Guerre, C. Taplan, R. Nicolaÿ, J.M. Winne, F.E. Du Prez, Fluorinated vitrimer elastomers with a dual temperature response, J. Am. Chem. Soc. 140 (2018) 13272–13284, https://doi.org/10.1021/jacs.8b07094.
[47] O. Anaya, A. Jourdain, I. Antoniuk, H. Ben Romdhane, D. Montarnal, E. Drockenmuller, Tuning the viscosity profiles of high- T_g poly(1,2,3-triazolium) covalent adaptable networks by the chemical structure of the N-substituents, Macromolecules 54 (2021) 3281–3292, https://doi.org/10.1021/acs.macromol.0c02221.
[48] D.J. Fortman, J.P. Brutman, C.J. Cramer, M.A. Hillmyer, W.R. Dichtel, Mechanically activated, catalyst-free polyhydroxyurethane vitrimers, J. Am. Chem. Soc. 137 (2015) 14019–14022, https://doi.org/10.1021/jacs.5b08084.
[49] J.O. Holloway, C. Taplan, F.E. Du Prez, Combining vinylogous urethane and β-amino ester chemistry for dynamic material design, Polym. Chem. 13 (2022) 2008–2018, https://doi.org/10.1039/D2PY00026A.
[50] N. Van Herck, D. Maes, K. Unal, M. Guerre, J.M. Winne, F.E. Du Prez, Covalent adaptable networks with tunable exchange rates based on reversible thiol–yne cross-linking, Angew. Chem. Int. Ed. 59 (2020) 3609–3617, https://doi.org/10.1002/anie.201912902.
[51] M. Podgórski, N. Spurgin, S. Mavila, C.N. Bowman, Mixed mechanisms of bond exchange in covalent adaptable networks: monitoring the contribution of reversible exchange and reversible addition in thiol–succinic anhydride dynamic networks, Polym. Chem. 11 (2020) 5365–5376, https://doi.org/10.1039/D0PY00091D.
[52] C. Taplan, M. Guerre, F.E. Du Prez, Covalent adaptable networks using β-amino esters as thermally reversible building blocks, J. Am. Chem. Soc. 143 (2021) 9140–9150, https://doi.org/10.1021/jacs.1c03316.
[53] L. Stricker, C. Taplan, F.E. Du Prez, Biobased, creep-resistant covalent adaptable networks based on β-amino ester chemistry, ACS Sustainable Chem. Eng. 10 (2022) 14045–14052, https://doi.org/10.1021/acssuschemeng.2c04822.
[54] D. Berne, B. Quienne, S. Caillol, E. Leclerc, V. Ladmiral, Biobased catalyst-free covalent adaptable networks based on CF_3 -activated synergistic aza-Michael exchange and transesterification, J. Mater. Chem. A 10 (2022) 25085–25097, https://doi.org/10.1039/D2TA05067F.
[55] D. Berne, G. Coste, R. Morales-Cerrada, M. Boursier, J. Pinaud, V. Ladmiral, S. Caillol, Taking advantage of β-hydroxy amine enhanced reactivity and functionality for the synthesis of dual covalent adaptable networks, Polym. Chem. 13 (2022) 3806–3814, https://doi.org/10.1039/D2PY00274D.
[56] G. Lee, H.Y. Song, S. Choi, C.B. Kim, K. Hyun, S. Ahn, Harnessing β-hydroxyl groups in poly(β-amino esters) toward robust and fast reprocessing covalent adaptable networks, Macromolecules 55 (2022) 10366–10376, https://doi.org/10.1021/acs.macromol.2c01872.
[57] S. Engelen, F. Van Lijsebetten, R. Aksakal, J.M. Winne, F.E. Du Prez, Enhanced viscosity control in thermosets derived from epoxy and acrylate monomers based on thermoreversible aza-michael chemistry, Macromolecules (2023), https://doi.org/10.1021/acs.macromol.3c01198 acs.macromol.3c01198.
[58] A.S. Angeloni, M. Laus, C. Castellari, G. Galli, P. Ferruti, E. Chiellini, Liquid crystalline poly(β-aminoester)s containing different mesogenic groups, Makromol. Chem. 186 (1985) 977–997, https://doi.org/10.1002/macp.1985.021860508.
[59] K. Kim, Y. Guo, J. Bae, S. Choi, H.Y. Song, S. Park, K. Hyun, S. Ahn, 4D printing of hygroscopic liquid crystal elastomer actuators, Small 17 (2021) 2100910, https://doi.org/10.1002/smll.202100910.
[60] T.H. Ware, M.E. McConney, J.J. Wie, V.P. Tondiglia, T.J. White, Voxelated liquid crystal elastomers, Science 347 (2015) 982–984, https://doi.org/10.1126/science.1261019.
[61] Q. Chen, W. Li, Y. Wei, Y. Ji, Reprogrammable 3D liquid-crystalline actuators with precisely controllable stepwise actuation, Adv. Intell. SystS. 3 (2021) 2000249, https://doi.org/10.1002/aisy.202000249.
[62] A. Ismagilova, L. Matt, P. Jannasch, V. Kisand, L. Vares, Ecotoxicity of isosorbide acrylate and methacrylate monomers and corresponding polymers, Green Chem. 25 (2023) 1626–1634, https://doi.org/10.1039/D2GC04178B.
[63] E. Yoshii, Cytotoxic effects of acrylates and methacrylates: relationships of monomer structures and cytotoxicity, J. Biomed. Mater. Res. 37 (1997) 517–524, https://doi.org/10.1002/(SICI)1097-4636(19971215)37:4<517::AID-JBM10>3.0.CO, 2-5.
[64] W. Xi, H. Peng, A. Aguirre-Soto, C.J. Kloxin, C.N. Bowman, Spatial and Temporal Control of Thiol-Michael Addition via Photocaged Superbase in Photopatterning and Two-Stage Polymer Networks Formation, 2014.
[65] B.D. Mather, K. Viswanathan, K.M. Miller, T.E. Long, Michael addition reactions in macromolecular design for emerging technologies, Prog. Polym. Sci. 31 (2006) 487–531, https://doi.org/10.1016/j.progpolymsci.2006.03.001.
[66] F. Van Lijsebetten, K. De Bruycker, E. Van Ruymbeke, J.M. Winne, F.E. Du Prez, Characterising different molecular landscapes in dynamic covalent networks, Chem. Sci. 13 (2022) 12865–12875, https://doi.org/10.1039/D2SC05528G.